BBA - Biomembranes 1866 (2024) 184367

Contents lists available at ScienceDirect

BBA - Biomembranes

journal homepage: www.elsevier.com/locate/bbamem

The molecular determinants of calcium ATPase inhibition by curcuminoids

Stefan Paula *, Sergiu Floruta, Karim Pajazetovic, Sydni Sobota, Dina Almahmodi

Department of Chemistry, California State University Sacramento, 6000 J Street, Sacramento, CA 95819, USA

ARTICLE INFO

Keywords:
Curcumin
Ligand docking
Sarco/endoplasmic reticulum calcium ATPase
Coupled enzyme inhibition assay
Inhibitor binding site, inhibitory potency, tryptophan fluorescence quenching

ABSTRACT

The natural product curcumin and some of its analogs are known inhibitors of the transmembrane enzyme sarco/endoplasmic reticulum calcium ATPase (SERCA). Despite their widespread use, the curcuminoids' binding site in SERCA and their relevant interactions with the enzyme remain elusive. This lack of knowledge has prevented the development of curcuminoids into valuable experimental tools or into agents of therapeutic value. We used the crystal structures of SERCA in its E1 conformation in conjunction with computational tools such as docking and surface screens to determine the most likely curcumin binding site, along with key enzyme/inhibitor interactions. Additionally, we determined the inhibitory potencies and binding affinities for a small set of curcumin analogs. The predicted curcumin binding site is a narrow cleft in the transmembrane section of SERCA, close to the transmembrane/cytosol interface. In addition to pronounced complementarity in shape and hydrophobicity profiles between curcumin and the binding pocket, several hydrogen bonds were observed that were spread over the entire curcumin scaffold, involving residues on several transmembrane helices. Docking-predicted interactions were compatible with experimental observations for inhibitory potencies and binding affinities. Based on these findings, we propose an inhibition mechanism that assumes that the presence of a curcuminoid in the binding site arrests the catalytic cycle of SERCA by preventing it from converting from the E1 to the E2 conformation. This blockage of conformational change is accomplished by a combination of steric hinderance and hydrogen-bond-based cross-linking of transmembrane helices that require flexibility throughout the catalytic cycle.

1. Introduction

Curcumin, a diarylheptanoid, is a natural product found in turmeric plants. It has a long history of use as a spice, herbal supplement, or therapeutic agent in alternative medicine [1–3]. The compound was first isolated in 1815 from rootstalks of turmeric plants [4]. About 100 years later, its chemical structure was determined and a route for its synthesis was devised shortly thereafter [5,6]. More recently, curcumin has attracted attention as a potential drug against a wide variety of medical conditions because of its anti-inflammatory, antibacterial, antifungal, and antimalarial properties [1,2,7]. It is also believed to be potentially beneficial for the treatment of cancer and Parkinson's disease [8–10]. Many of curcumin's perceived or confirmed therapeutic benefits stem from its antioxidant properties and its ability to interfere with calcium signaling. It has been proposed that latter is, at least in part, the result of curcumin-mediated inhibition of the transmembrane enzyme sarco/endoplasmic reticulum calcium ATPase (SERCA)[1] [11–13].

SERCA belongs to the family of P-type ATPases and resides in the membrane of the sarco/endoplasmic reticulum [14–18]. It keeps intracellular calcium concentrations low by using chemical energy obtained from the hydrolysis of ATP to expel calcium ions from the cytosol and release them into the lumen of the sarco- or endoplasmic reticulum, both of which serve as intracellular calcium storage compartments. The rapid release of calcium ions from these reservoirs triggers a variety of physiologically critical processes, such as muscle contraction, which accounts for SERCA's central role in calcium-signaling pathways. Its catalytic cycle is commonly described in terms of the Post-Albers scheme (Fig. 1) that is based upon SERCA undergoing significant conformational changes, involving interconversions between the so-called E1 and E2 main conformations of the enzyme, each of which exists in distinct

* Corresponding author.
E-mail address: stefan.paula@csus.edu (S. Paula).

[1] Abbreviations: ATP: adenosine triphosphate; BHQ: di-*tert*-butyl hydroquinone; CPA: cyclopiazonic acid; GBVI/WSA: generalized Born volume integral/weighted surface area; LDH: lactate dehydrogenase; MOE: molecular operating environment; MOPS: 3-(N-morpholino)-propanesulfonic acid; PK: pyruvate kinase; PLB: propensity for ligand binding; SAR: structure-activity relationship; SERCA: sarco/endoplasmic reticulum calcium ATPase; TG: thapsigargin; TM: transmembrane helix; TRIS: tris(hydroxymethyl)aminomethane.

https://doi.org/10.1016/j.bbamem.2024.184367
Received 1 February 2024; Received in revised form 4 June 2024; Accepted 1 July 2024
Available online 3 July 2024
0005-2736/

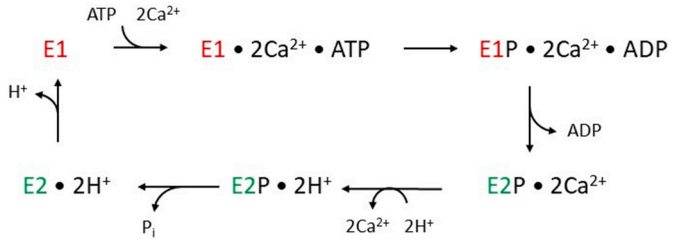

Fig. 1. Post-Albers scheme, showing the conformational changes that SERCA undergoes during its catalytic cycle. The various E1 conformations are shown in red and the E2 conformations in green. (For interpretation of the references to colour in this figure legend, the reader is referred to the web version of this article.)

substates [19,20]. Briefly, the cycle begins with SERCA binding two calcium ions on the cytosolic side of the SR/ER membrane and one molecule of ATP in its E1 conformation before one of its aspartic acid residues becomes phosphorylated. Phosphorylation occludes the cytosolic calcium binding sites and subsequently triggers the conversion to the E2 conformation, which expels both calcium ions into the lumen and leads to the uptake of two protons. Subsequent hydrolysis of the phosphate group then resets the cycle as SERCA reverts to the E1 form, accompanied by the release of two protons on the cytosolic side (Fig. 1).

In vivo, SERCA activity is regulated by endogenous inhibitors, such as the short peptides phospholamban and sarcolipin [21–23]. In addition to these regulatory peptides, a broad variety of exogenous compounds are also capable of interfering with the ion-transport activity of SERCA [11,24,25]. Well-known examples are the natural product thapsigargin (TG) and its derivatives, the fungal metabolite cyclopiazonic acid (CPA), or the small compound di-*tert*-butyl hydroquinone (BHQ), all of which are allosteric inhibitors that are known to bind to the transmembrane domain of SERCA [26–28]. The value of SERCA inhibitors as research tools or as potential drug candidates is well-documented by an impressively large number of publications. For example, derivatives of TG have undergone clinical trials as prodrugs for the treatment of prostate cancer, solid tumors, and glioblastomas [29–32].

To carry out its catalytic function, SERCA needs to be able to interconvert freely between its various E1 and E2 conformations depicted in Fig. 1 [19,20]. Most but not all allosteric SERCA inhibitors interfere with catalysis by binding to the enzyme and preventing further conformational changes, thus arresting it in its E2 conformation and blocking the binding of cytosolic calcium ions [18,33]. For some of the most commonly used inhibitors, high resolution X-ray crystal structures of the inhibitor/SERCA complex in various conformations are available that have elucidated inhibitor binding at the molecular level [34–36]. These studies have shown that all allosteric SERCA inhibitor binding sites reside in the enzyme's transmembrane domain, an observation that is consistent with the overall hydrophobic character of these compounds.

Curcumin belongs to the relatively small group of SERCA inhibitors that has a preference for binding to the E1 over the E2 form of the enzyme [11,12]. A calculated log *P* value of about 3.8 implies a predominantly hydrophobic character and suggests a binding site within the transmembrane section of SERCA, even though a previous study has proposed a lumenal site in the E2 form as the presumed binding pocket for a synthetic curcumin analog [37]. At present, no high-resolution structure of the curcumin/SERCA complex is available which would clearly reveal location and structure of the binding site. In addition, no comprehensive structure-activity relationship (SAR) studies have been conducted, which would have assisted in the identification of the curcumin binding site indirectly by characterizing critical enzyme/inhibitor interactions. In fact, only a few publications are available that report the activities for a limited number of curcuminoids and their results are not always compatible with each other [13,38].

Here, we employed computational tools in combination with traditional inhibition and binding assays to identify the most likely binding site of curcumin to SERCA and to characterize intermolecular interactions relevant for binding. To achieve this goal, we screened the crystal structure of SERCA in two representative E1 conformations for viable binding sites and then employed molecular docking and molecular mechanics to find the most probable inhibitor binding mode, along with the relevant enzyme/inhibitor interactions. As the most feasible binding site, we identified a cleft in the transmembrane section of the enzyme that displays pronounced shape complementarity with curcumin and that is only present in the E1 conformation. The predicted interactions were consistent with experimentally observed trends in inhibitory potencies and binding affinities that we measured for a small collection of curcumin analogs. As a plausible inhibition mechanism, we propose that curcumin hinders SERCA's E1 to E2 conversion by a combination of steric blockage of the enzyme's conformational switch and by cross-linking several transmembrane helices through a network of hydrogen bonds that are mediated by the inhibitor.

2. Methods

2.1. Molecular modeling and computation

The three-dimensional molecular structure of curcumin was sketched using the comprehensive modeling suite MOE (Molecular Operating Environment, version 2019.0102; Chemical Computing Group, Montreal, Canada). In agreement with an NMR study, the enol tautomer (Fig. 2) was chosen over the diketone form as the more stable and thus representative isomer of the molecule [39]. The conformational energy of the model was then minimized by molecular mechanics using the MMFF94x force field, which is widely regarded a suitable choice for small organic molecules.

Several X-ray crystal structures of SERCA were obtained from the Protein Databank. As representatives for the E1 conformation, an ATP-free conformation and one with an ATP analog (PDB IDs: 1SU4 and 1VFP, respectively [40,41]) were chosen. SERCA complexed with beryllium trifluoride was selected as a representative form of the E2 conformation (PDB ID: 3B9B) [42]. All structures were prepared in MOE for further analysis by removing solvent and buffer molecules, adding hydrogen atoms, and optimizing their positions by molecular mechanics in conjunction with the Amber force field as implemented in the Structure Preparation functionality of MOE.

The surfaces of the three SERCA conformations were screened for potential binding sites with the SiteFinder tool in MOE [43]. Potential sites were evaluated based on their size, location, and their PLB (propensity for ligand binding) score [44]. Next, the structural model of curcumin was docked into some of these sites by employing MOE's Dock tool executed at the default settings [45]. Curcumin/SERCA complexes obtained from docking were subjected to a brief energy optimization by molecular mechanics using the Amber forcefield to relieve potential conformational strain in the receptor that was not relieved during docking. For the visualization of docked inhibitor poses, two-dimensional projections of the ligand in the binding pocket were created with the Ligand Interactions feature of MOE.

2.2. Materials

Muscle tissue from rabbit hind legs for the preparation of microsomes was a gift from a local breeder. An enzyme mixture of pyruvate kinase (PK) and lactate dehydrogenase (LDH) and the compounds dimethoxycurcumin (**4**), tetramethylcurcumin (**5**), 1,5-bis(3,5-dimethoxyphenyl)-1,4-pentadien-3-one (**6**), and vanillylidenacetone (**8**) were received from Sigma-Aldrich (St. Louis, MO). Curcumin (**1**), demethoxycurcumin (**2**), bisdemethoxycurcumin (**3**), ferulic acid (**7**) and all other reagents for the assays were obtained from Fisher Scientific (Waltham, MA).

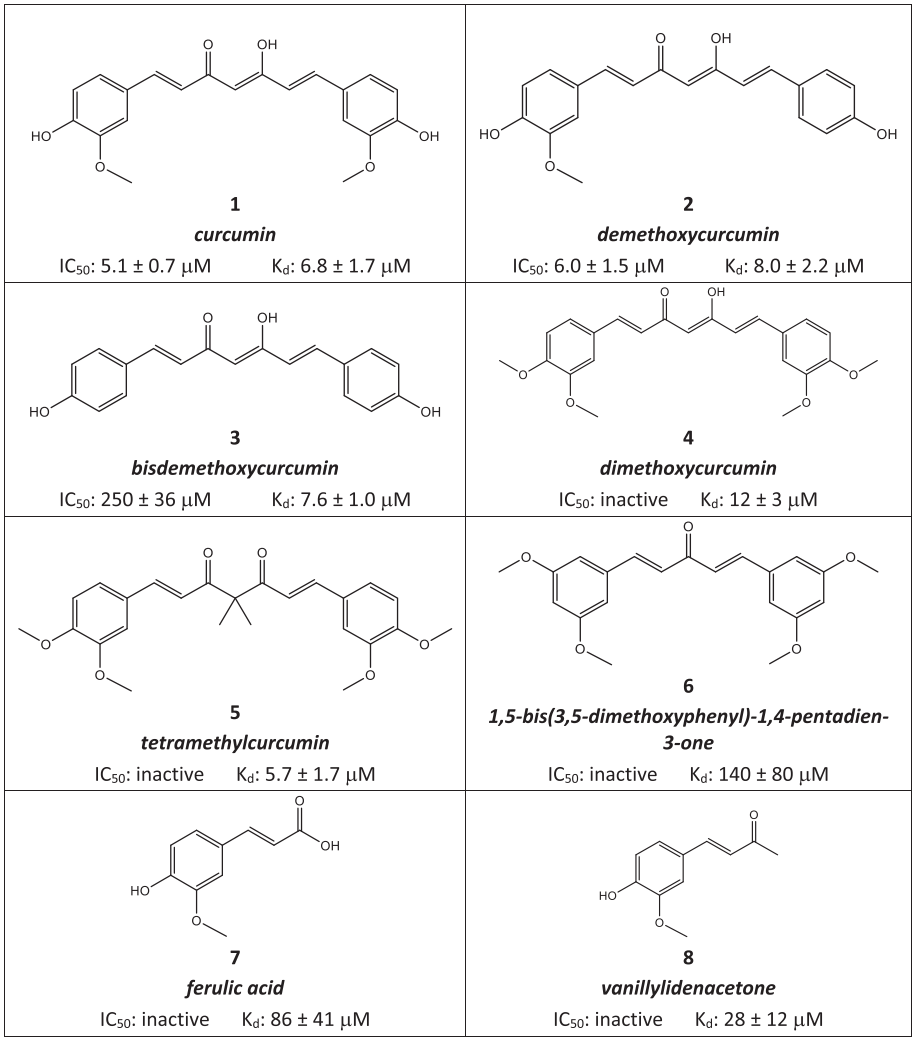

Fig. 2. Chemical structure, inhibitory potencies, and binding affinities of curcuminoids.

2.3. SERCA activity assays

SERCA microsomes from rabbit hind leg tissue were prepared according to a previously described procedure [46,47]. SERCA-catalyzed rates of ATP hydrolysis coupled to the oxidation of NADH by the action of the auxiliary enzymes PK and LDH were measured spectroscopically using a Biotek Synergy HTX microplate reader (Agilent, Santa Clara, CA) operating at a wavelength of 340 nm [46]. Briefly, ATP hydrolysis was initiated in samples placed in the wells of 96-well plates by the addition of ATP to give a final concentration of 0.22 mM. Each well contained a total volume of 225 μL, containing 8 μg/mL total protein in assay buffer (5 mM $MgCl_2$, 100 mM KCl, 0.7 mM $CaCl_2$, 0.5 mM EGTA, 5.5 μM calcimycin, 1.5 mM phosphoenolpyruvate, and 20 mM tris (hydroxymethyl)aminomethane (Tris) at pH 7.3). Reaction rates were measured for five minutes at 11 different test compound concentrations that covered a concentration range that was evenly spaced on a logarithmic scale between 5.6 nM and 330 μM. The observed rates were then fit to a three-parameter logistic equation using SigmaPlot (version 14.5, Systat Software). Inhibitory potencies were expressed in terms of the IC_{50} value, the inhibitor concentration that reduced SERCA activity by 50 % [48]. Reported potencies and their standard deviations were calculated by averaging the IC_{50} values obtained from at least three independent repeats.

2.4. Tryptophan fluorescence quenching assays

Measurement of tryptophan fluorescence quenching due to inhibitor binding was performed using a previously established protocol [49]. 3 mL samples of SERCA microsomes were suspended at a total protein concentration of 94 μg/mL in assay buffer that forced the enzyme into the E1 conformation (50 mM KCl, 5 mM $MgCl_2$, 50 μM $CaCl_2$, and 50 mM 3-(N-morpholino)propanesulfonic acid (MOPS) at pH 7.2) in a stirred quartz cuvette. Fluorescence was measured with a fluorimeter Shimadzu (RF-6000) operating at an excitation wavelength of 295 nm, an emission wavelength of 335 nm, and slit widths of 5 nm and 10 nm for excitation and emission, respectively. Measurements were performed at six test compound concentrations between 200 nM to 625 μM that were equally spaced on a logarithmic scale. Samples were allowed to equilibrate for 5 min, after which fluorescence intensities were recorded. Binding constants were obtained by graphing the absolute decrease in fluorescence intensity against the test compound concentration and fitting the data to a single-site binding curve using SigmaPlot. Runs for each curcuminoid were performed at least in triplicate and binding affinities were expressed as the average dissociation constants (K_d) with standard deviations obtained from a minimum of three independent trials.

3. Results and discussion

3.1. Computationally identified binding site and curcumin/SERCA interactions

As curcumin has been shown to bind to SERCA in the enzyme's E1 conformation, the surface of corresponding high-resolution X-ray crystal structures were examined for potential binding sites with the SiteFinder tool implemented in MOE. Since it is not known to which E1 substate the inhibitor binds, we selected two forms as representatives: an ATP-free form (1SU4) and one containing an ATP analog (1VFP). In the case of 1SU4, only three potential sites were large enough to accommodate a ligand approximately the size of curcumin that also had high PLB scores and that were located inside or close to the transmembrane domain (Fig. 3, left panel). The largest of these sites was located at the membrane/cytosol interface (site 1), a wide and diffuse area that did not reveal a single consensus binding site and that was therefore not considered further. A second, more discrete site was identified at the opposite side of the transmembrane domain of SERCA, sandwiched between the short lumenal loops that connect transmembrane helices (TM) TM1 with TM2 and TM3 with TM4, respectively (site 2). A third site was found in SERCA's transmembrane domain, close to the membrane/cytosol interface in an area bordering helices TM1–4 (site 3). Interestingly, site 3 was in the vicinity of the binding sites of BHQ and CPA [50,51], even though these two inhibitors have been shown to bind to E2 rather than to E1. These three sites were also present in 1VFG, the structure of SERCA in complex with an ATP analog, albeit with slightly different sizes and minor shifts in their location (Fig. 3, center panel). For example, site 1 was somewhat smaller in comparison and site 3 extended slightly more toward the cytosol/membrane interface.

Only sites 2 and 3 were considered for further evaluation. The structure of curcumin was docked into these sites in both E1 conformations and the poses with the highest docking scores of each were then subjected to a brief energy optimization by molecular mechanics and rescored. Both sites showed rather favorable binding interactions in that they were affiliated with large and negative values for the docking score implemented in MOE, expressed as the "S-value". The latter represents the GBVI/WSA (generalized-Born volume integral/weighted surface area) binding free energy that serves as a numerical measure for binding affinity, [45]. Even though the top-ranked curcumin poses for site 2 had somewhat more favorable docking scores than the ones obtained for site 3 in both E1 conformations (1SU4: S = −9.45 versus S = −8.62; 1VFP: S = −9.47 versus S = −8.21), site 3 appeared the more likely binding site candidate for reasons stated below. It is also interesting to note that the differences in scores between 1SU4 and 1VFP for both sites were relatively minor, suggesting that curcumin may be able to bind to both conformations with similar affinity.

Docking curcumin into site 3 of the two E1 conformations yielded very similar curcumin poses with the 1VFP pose slightly shifted toward the cytosolic interface in comparison to 1SU4. However, in both conformations, site 3 comprises a narrow, elongated cleft on SERCA's surface that, unlike site 2, has excellent shape complementarity with curcumin (Fig. 4, upper panels), facilitating a snug fit of the inhibitor. Due to an abundance of close contacts, van-der-Waals interactions are likely a major contributor to the binding energy. Moreover, the hydrophobicity profile of curcumin matches that of the binding site, with curcumin's two phenyl rings and the hydrocarbon parts of the linker seen in close proximity of nonpolar patches (Fig. 4, lower panels). This suggests that hydrophobic interactions are another driver of inhibitor binding. Docking simulations also identified several hydrogen bonds as factors aiding inhibitor binding (Fig. 5). Unlike in site 2, these interactions are distributed over the entire curcumin scaffold and involve several residues that are part of three transmembrane helices of SERCA. Both ring hydroxyl groups of curcumin act as hydrogen bond donors, connecting with Glu309 and Thr316 (both on TM4) in the case of 1SU4 and with Asn56 (TM1) and Arg 304 (TM4) in the case of 1VFP. Interestingly, Glu309 has been identified as one of the calcium-coordinating residues with a proposed gating function [52]. Its interaction with curcumin could potentially impair its ability to participate in calcium transport, thereby contributing to inhibition. In addition, the hydroxyl group in the linker section of curcumin in 1SU4 was predicted to act as a hydrogen bond donor with Glu109 (TM2) and one of the phenyl hydrogen atoms was engaged in an aromatic hydrogen bond with Glu51 (TM1). Overall, the placement of curcumin in site 3 instead of site 2 allowed for a wider range of intermolecular interactions and facilitated are more effective interference with SERCA's catalytic cycle (see section 3.3). Lastly, the location of site 3 in the transmembrane SERCA domain is compatible with curcumin's overall hydrophobic nature (log P of 3.8 as calculated in MOE) and with previous structural studies that placed the sites of several other SERCA inhibitors (TG, CPA, and BHQ) in that area [28,50].

3.2. SARs from inhibition and binding assays

Among the eight curcuminoids tested, only three revealed detectable inhibitory activities (Fig. 2). In the SERCA inhibition assays (see Fig. 6,

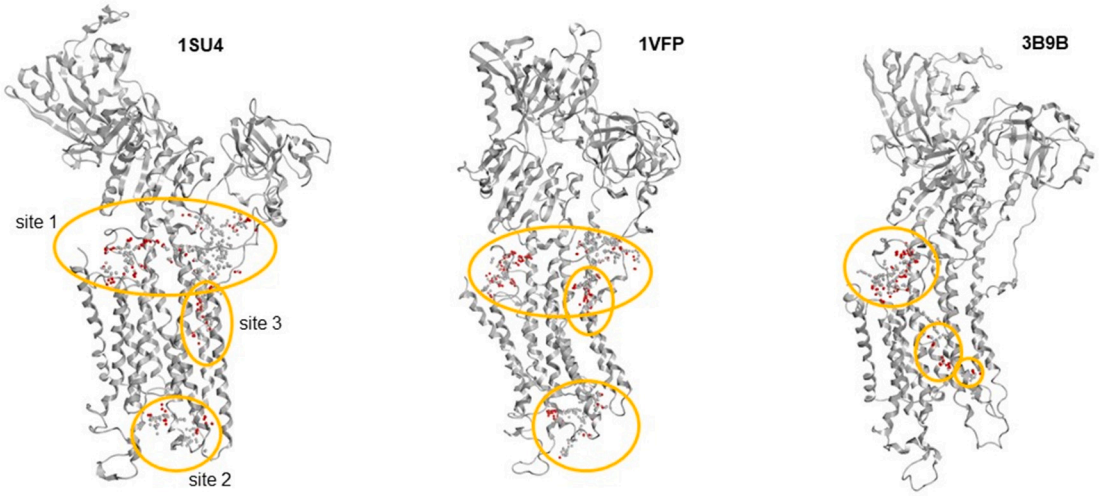

Fig. 3. Potential inhibitor binding sites identified by SiteFinder in MOE at the cytosol/transmembrane interface (site 1), at the lumen/transmembrane interface (site 2), and in the transmembrane domain (site 3). Displayed are X-ray crystal structures of SERCA in the E1•2Ca^{2+} (1SU4, left), E1•2Ca^{2+}•AMPPCP (1VFP, center), and the E2•BeF_3 (3B9B, right) conformations.

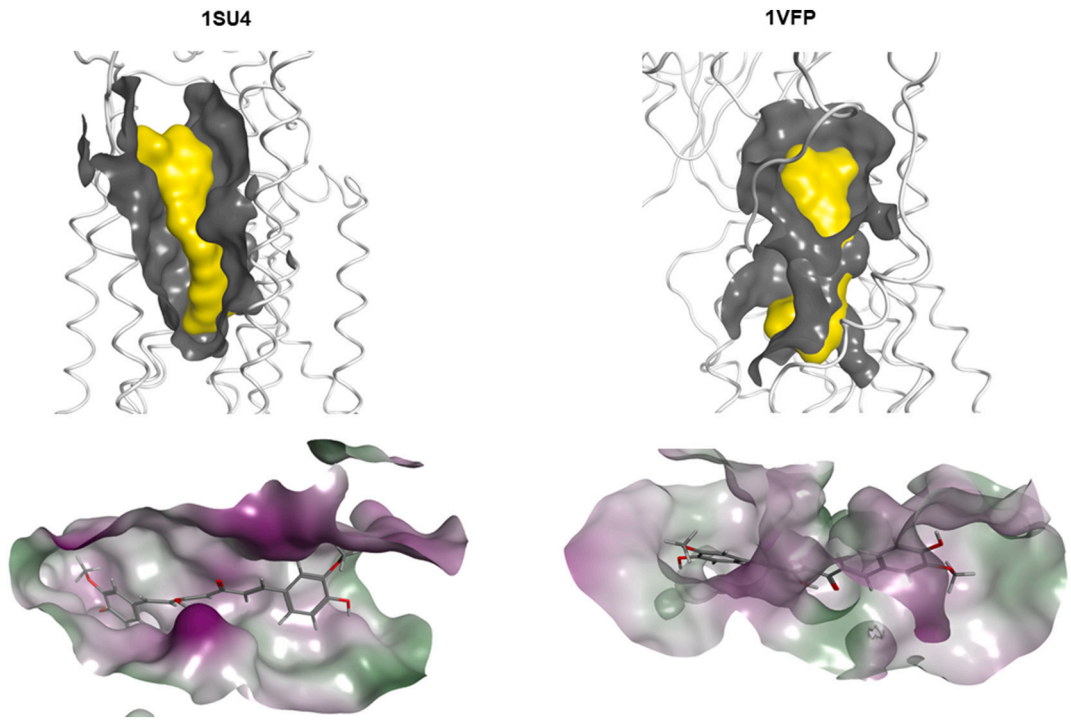

Fig. 4. Upper panel: Shape complementarity between the predicted curcumin binding site (grey) and the docked inhibitor (yellow). Lower panel: Hydrophobicity profile of the binding pocket's surface (purple: hydrophilic, green hydrophobic) with docked inhibitor (sticks). (For interpretation of the references to colour in this figure legend, the reader is referred to the web version of this article.)

left panel, for two representative curves), the parent compound curcumin (**1**) displayed an IC_{50} value of 5.1 μM, which is in excellent agreement with previously reported potencies [12,13,38,53]. Removal of one of the ring methoxy groups (demethoxycurcumin, **2**) did not affect potency within experimental error (IC_{50}: 6.1 μM). This observation suggests that one of the two methoxy group is not needed for inhibition, a finding that is compatible with the docking results (Fig. 5). Removal of both methoxy groups (bisdemethoxycurcumin, **3**), however, resulted in a noticeable drop in potency (IC_{50}: 250 μM), suggesting that one of curcumin's two methoxy groups is required for effective inhibition, which is also suggested by the docking simulations. Both observations are compatible with a report by Dao and coworkers [38], whereas the reduced potency of **3** does not agree with the results of Logan-Smith [13]. The inactivity of compounds **4**–**6** highlights the importance of the hydroxyl groups for potency. Moreover, the additional steric bulk present at the center of the linker in the form of the two additional methyl groups in **5** may impede this compound's activity. Furthermore, the two methyl groups force the compound to adopt a diketone tautomer, which changes the hydrogen bond pattern in the center of the molecule in comparison to the active compounds **1**–**3**. The inactivity of the shorter **6** and the single-ring curcuminoids **7** and **8** emphasizes the need for two rings placed at a proper distance from each other.

The binding assays based on fluorescence quenching of tryptophan residues in SERCA's transmembrane domain yielded measurable affinities for all compounds tested (Fig. 2 and Fig. 6, right panel, for two representative binding curves). In agreement with the inhibition assays, the two most active inhibitors, compounds **1** and **2**, also had the highest binding affinities (K_d of 6.8 and 8.0 μM, respectively). Somewhat surprisingly, compounds **3**–**5** (poor inhibitors or inactive compounds) also displayed binding affinities in the low micromolar range, albeit with a slightly larger K_d value in the case of **4**. Apparently, their structural resemblance with **1** and **2** allows them to bind to SERCA, but they lack the ability to engage in some of the interactions required for interfering with the enzyme's catalytic cycle, such as hydroxyl groups capable of forming hydrogen bonds (**4** and **5**). The remaining three compounds all showed reduced affinities, particularly **6**. A probable reason for the latter relates to the nature of the linker that connects the phenyl groups, which is shorter by two carbon atoms in comparison to **1**–**5**. This places the two bulky phenyl groups in closer proximity, a scenario that likely introduces steric clashes in the binding site which is highly complementary to the shape of the larger curcuminoids. The two smallest compounds, **7** and **8**, had intermediate affinities (K_d of 86 and 28 μM, respectively), which is compatible with them occupying "half" of the binding site. Since inhibition requires interactions with residues across the entire binding site, however, they fail to inhibit SERCA.

3.3. *A proposed mechanism for curcumin-based SERCA inhibition*

As an allosteric inhibitor, curcumin fundamentally differs from a competitive inhibitor in that it binds to SERCA at a location different from an active site, such as the ATP binding pocket. Whereas good binding affinity for the target remains a necessary requirement for effective inhibition, it is not a sufficient one. Once bound, an allosteric inhibitor also needs to block the interconversion between the various enzyme conformations that are part of the catalytic cycle. Below, we present two scenarios that describe how this may occur in the case of curcuminoids inhibiting SERCA.

Maybe the most straightforward account is that the docking-predicted hydrogen bonds that involve residues residing on three different transmembrane helices of SERCA (Glu51 and Asn56 on TM1, Glu 109 on TM2, and Arg 334, Glu309, and Thr316 on TM4) limit helix mobility via cross-linking. It has been shown that the conformational change from E1 to E2 involves large-scale movements of SERCA's helices, which would be hindered by the presence of these hydrogen bonds [35]. This notion is supported by the observation that only the larger curcuminoids that form hydrogen bonds with multiple helices are active.

Another plausible scenario also supported by the docking simulations is that curcumin's tight fit into the binding cleft in the E1 form prevents the enzyme's transition into the E2 conformation by the steric

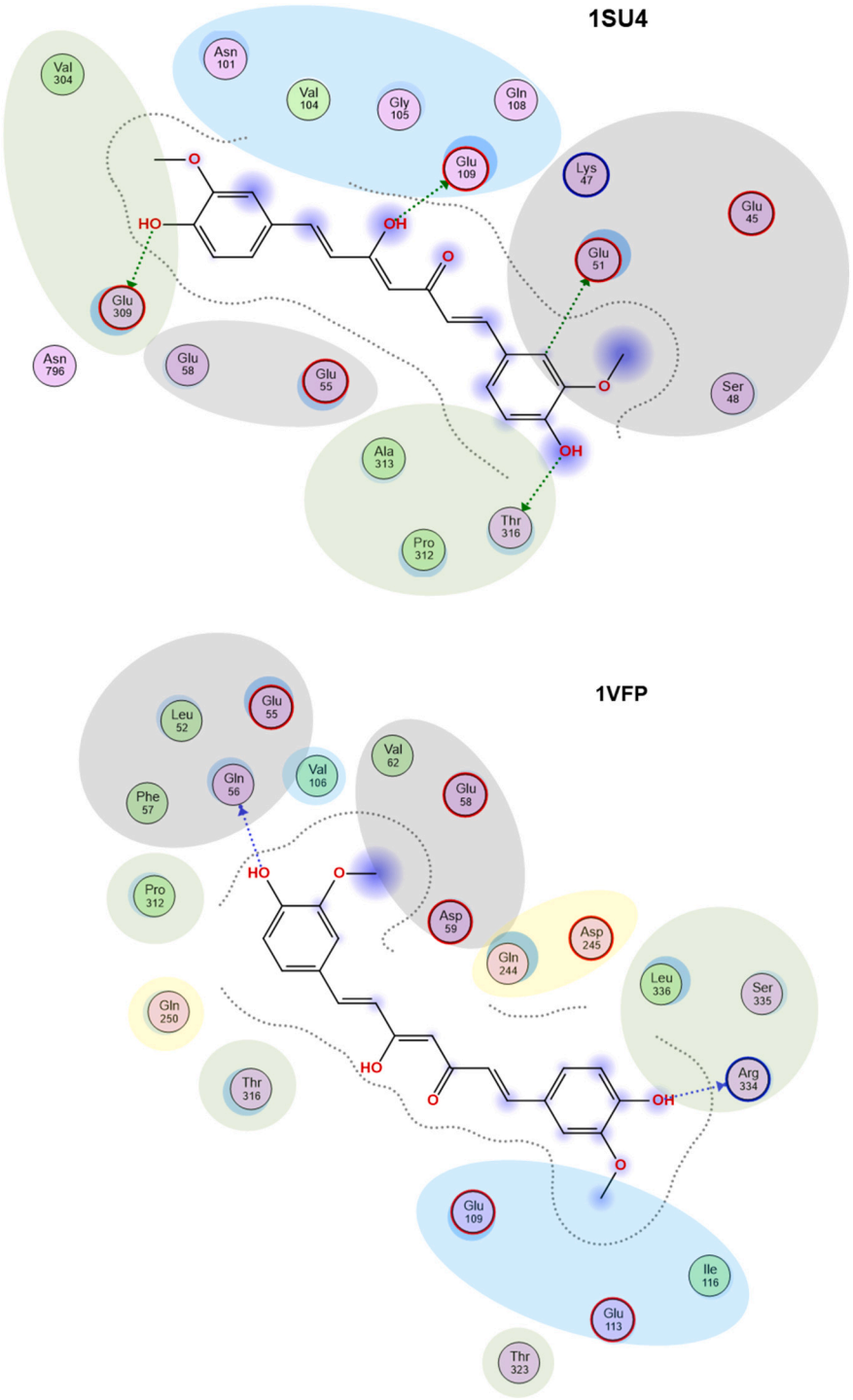

Fig. 5. Docking-predicted curcumin/SERCA interactions. Broken lines indicate hydrogen-bonds. Non-polar residues are displayed in green whereas polar ones are displayed in purple. Grey, blue yellow, and green backgrounds identify residues that are part of TM1, TM2, TM3, and TM4, respectively. (For interpretation of the references to colour in this figure legend, the reader is referred to the web version of this article.)

collisions that would result from such a conformational change. This is easily visualized by an inspection of Fig. 3 (right panel) that shows that the E2 conformation lacks a binding site located in the area corresponding to site 3 of the E1 conformation that would be suitable for curcumin binding. As a result, SERCA is unable to convert from E1 to E2 with curcumin bound to it, thereby effectively arresting the enzyme's catalytic cycle.

Alternatively, a superposition of the residues forming the binding site of the enzyme/curcumin complex onto their counterparts in the E2 conformation reveals that the presence of the inhibitor constitutes a serious obstacle for the E1-to-E2 conversion (Fig. 7, upper panel). Even though such a superposition is imperfect due to the stark conformational differences between E1 and E2, it shows that the inhibitor likely causes steric clashes with the enzyme that are distributed over the entire length of the binding site. Thus, the transition to E2 in the inhibitor's presence would require a substantial amount of flexibility that may be difficult to overcome, even for a protein such as SERCA that has been shown to possess great flexibility in its transmembrane domain [21]. A good

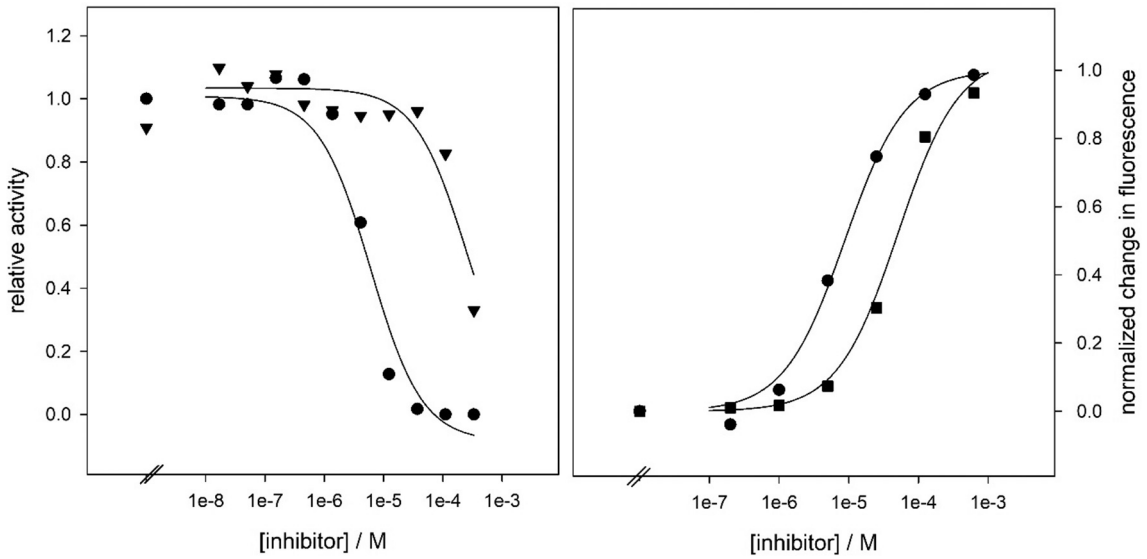

Fig. 6. Left panel: Representative SERCA activity inhibition data with fit curves for **1** (circles) and **3** (triangles). The uninhibited ATPase activity was 7.8 μmol/(min mg). Right panel: Representative tryptophan fluorescence quenching data with fit curves for **1** (circles) and **7** (squares).

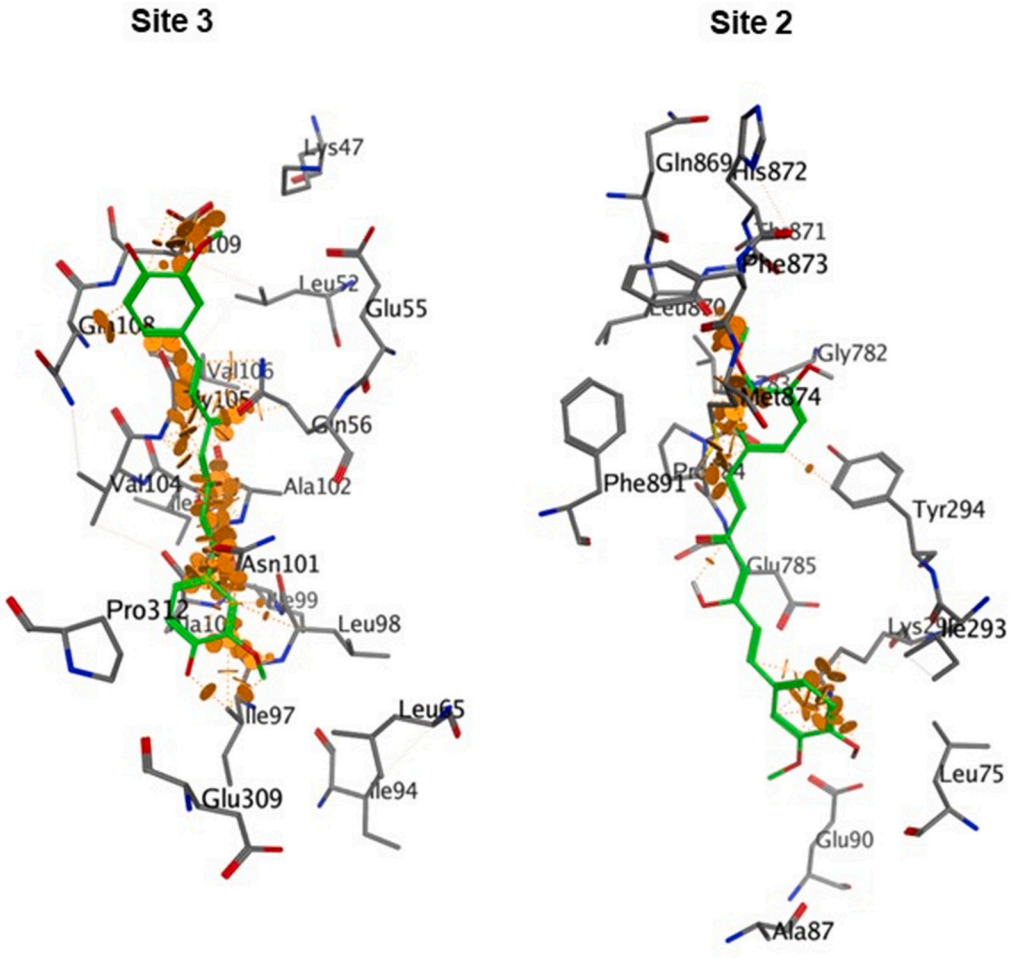

Fig. 7. Steric clashes between curcumin and SERCA created by the E1-to-E2 conformational transition. Orange disks indicate steric clashes in the transmembrane (left panel, site 3) and the lumenal (right panel, site 2) docking sites when the inhibitor is placed in the E2 (1SU4) conformation of SERCA.

example for the noticeable conformational flexibility of SERCA is the observation that inhibitors such as TG lock the enzyme's transmembrane domain without preventing ligand binding in the cytosolic domain [33]. It should be noted that the relatively high binding affinity of some of the shorter curcuminoids is not a contradiction of this scenario since their smaller sizes would result in fewer clashes that the enzyme might be able to overcome, allowing it to remain catalytically active.

Finally, we would like to point out that the proposed inhibition mechanism supports the choice of site 3 over the lumenal site 2 as the most likely curcumin binding site. An inspection of curcumin docked into site 2 in the E1 form and then superimposed onto the E2 conformation reveals a greatly reduced extent of steric clashes that would accompany a potential E1 to E2 conversion, making effective inhibition by steric blockage less likely (Fig. 7, lower panel). Moreover, from a mechanical point of view, inhibition via cross-linking of transmembrane helices via hydrogen bonds seems more effective if the connecting inhibitor resides inside the transmembrane domain close to the center of the helices (site 3), rather than at the two loops connecting the tips of helices TM1 with TM2 and TM3 and TM4, respectively (site 2).

4. Conclusions

In this study, we have identified the most plausible binding site of curcuminoids in SERCA and have characterized the molecular interactions between the enzyme and this particular inhibitor class. We accomplished this task by using a combination of experimental assays and molecular modeling techniques, a frequently employed avenue to obtain structural information in the absence of a high-resolution structure of an inhibitor/enzyme complex. The gained knowledge can serve broader purposes, such as a platform for future searches for novel inhibitors with different scaffolds that bind to the same site. In general, knowledge of the 3D structure of the targeted receptor's binding site is a considerable asset for the discovery of new bioactive compounds as it allows for the application of powerful structure-based methodologies to virtually screen large compound repositories [54]. Moreover, subsequent synthetic efforts to optimize the inhibitory potency and other physical properties of a hit compound would benefit from the availability of a structural model like the one presented here.

Funding

This work was supported in part by funds from the Center for Interdisciplinary Molecular Biology: Education, Research and Advancement (Sacramento State University) and in part by grants from the National Science Foundation (Award number 2327946 to S.P.) and the National Institute of General Medical Sciences (Award number 1 R16GM145435-01A1 to S.P.).

CRediT authorship contribution statement

Stefan Paula: Writing – review & editing, Writing – original draft, Supervision, Methodology, Investigation, Funding acquisition, Conceptualization. **Sergiu Floruta:** Investigation. **Karim Pajazetovic:** Investigation. **Sydni Sobota:** Investigation. **Dina Almahmodi:** Investigation.

Declaration of competing interest

The authors declare the following financial interests/personal relationships which may be considered as potential competing interests: Stefan Paula reports financial support was provided by National Institute of General Medical Sciences. Stefan Paula reports financial support was provided by National Science Foundation. If there are other authors, they declare that they have no known competing financial interests or personal relationships that could have appeared to influence the work reported in this paper.

References

[1] K.I. Priyadarsini, The chemistry of curcumin: from extraction to therapeutic agent, Molecules 19 (2014) 20091–20112.
[2] T. Esatbeyoglu, P. Huebbe, I.M. Ernst, D. Chin, A.E. Wagner, G. Rimbach, Curcumin - from molecule to biological function, Angew. Chem. International ed 51 (2012) 5308–5332.
[3] R.K. Maheshwari, A.K. Singh, J. Gaddipati, R.C. Srimal, Multiple biological activities of curcumin: a short review, Life Sci. 78 (2006) 2081–2087.
[4] H.A. Vogel, J. Pelletier, Curcumin - biological and medicinal properties, Aust. J. Pharm. 2 (1815) 50.
[5] V. Lampe, J. Milobedzka, Studien über Curcumin, Ber. Dtsch. Chem. Ges. 46 (1913) 2235–2240.
[6] V. Lampe, Synthese von curcumin, Ber. Dtsch. Chem. Ges. 51 (1918) 1347–1355.
[7] K.M. Nelson, J.L. Dahlin, J. Bisson, J. Graham, G.F. Pauli, M.A. Walters, The essential medicinal chemistry of curcumin, J. Med. Chem. 60 (2017) 1620–1637.
[8] A. Giordano, G. Tommonaro, Curcumin and cancer, Nutrients 11 (2019).
[9] Z. Rabiei, K. Solati, H. Amini-Khoei, Phytotherapy in treatment of Parkinson's disease: a review, Pharm. Biol. 57 (2019) 355–362.
[10] T. Jin, Y. Zhang, B.O.A. Botchway, J. Zhang, R. Fan, Y. Zhang, X. Liu, Curcumin can improve Parkinson's disease via activating BDNF/PI3k/Akt signaling pathways, Food Chem. Toxicol. 164 (2022) 113091.
[11] F. Michelangeli, J.M. East, A diversity of SERCA Ca^{2+} pump inhibitors, Biochem. Soc. Trans. 39 (2011) 789–797.
[12] J.G. Bilmen, S.Z. Khan, M.H. Javed, F. Michelangeli, Inhibition of the SERCA Ca^{2+} pumps by curcumin. Curcumin putatively stabilizes the interaction between the nucleotide-binding and phosphorylation domains in the absence of ATP, Eur. J. Biochem. 268 (2001) 6318–6327.
[13] M.J. Logan-Smith, P.J. Lockyer, J.M. East, A.G. Lee, Curcumin, a molecule that inhibits the Ca^{2+}-ATPase of sarcoplasmic reticulum but increases the rate of accumulation of Ca^{2+}, J. Biol. Chem. 276 (2001) 46905–46911.
[14] D.H. MacLennan, Purification and properties of an adenosine triphosphatase from sarcoplasmic reticulum, J. Biol. Chem. 245 (1970) 4508–4518.
[15] J.V. Moller, B. Juul, M. le Maire, Structural organization, ion transport, and energy transduction of P-type ATPases, Biochim. Biophys. Acta 1286 (1996) 1–51.
[16] J.V. Moller, P. Nissen, T.L. Sorensen, M. le Maire, Transport mechanism of the sarcoplasmic reticulum Ca^{2+}-ATPase pump, Curr. Opin. Struct. Biol. 15 (2005) 387–393.
[17] J.O. Primeau, G.P. Armanious, M.E. Fisher, H.S. Young, The sarco/endoplasmic reticulum calcium ATPase, Subcell. Biochem. 87 (2018) 229–258.
[18] J.V. Moller, C. Olesen, A.M. Winther, P. Nissen, The sarcoplasmic Ca^{2+}-ATPase: design of a perfect chemi-osmotic pump, Q. Rev. Biophys. 43 (2010) 501–566.
[19] R.W. Albers, Biochemical aspects of active transport, Annu. Rev. Biochem. 36 (1967) 727–756.
[20] X.C. Zhang, H. Zhang, P-type ATPases use a domain-association mechanism to couple ATP hydrolysis to conformational change, Biophys. Rep. 5 (2019) 167–175.
[21] M. Asahi, Y. Sugita, K. Kurzydlowski, S. De Leon, M. Tada, C. Toyoshima, D. H. MacLennan, Sarcolipin regulates sarco(endo)plasmic reticulum Ca^{2+}-ATPase (SERCA) by binding to transmembrane helices alone or in association with phospholamban, Proc. Natl. Acad. Sci. USA 100 (2003) 5040–5045.
[22] B.L. Akin, T.D. Hurley, Z. Chen, L.R. Jones, The structural basis for phospholamban inhibition of the calcium pump in sarcoplasmic reticulum, J. Biol. Chem. 288 (2013) 30181–30191.
[23] D.H. MacLennan, E.G. Kranias, Phospholamban: a crucial regulator of cardiac contractility, Nat. Rev. Mol. Cell Biol. 4 (2003) 566–577.
[24] S. Paula, Progress in the discovery of SERCA inhibitors, in: G.P.C.A.S. Ricci (Ed.), Medicinal Chemistry Research Progress, Nova Science Publishers, Inc., 2008.
[25] L. Peterkova, E. Kmonickova, T. Ruml, S. Rimpelova, Sarco/endoplasmic reticulum calcium ATPase inhibitors: beyond anticancer perspective, J. Med. Chem. 63 (2020) 1937–1963.
[26] M. Treiman, C. Caspersen, S.B. Christensen, A tool coming of age: thapsigargin as an inhibitor of sarco-endoplasmic reticulum Ca^{2+}-ATPases, Trends Pharmacol. Sci. 19 (1998) 131–135.
[27] Y.M. Khan, M. Wictome, J.M. East, A.G. Lee, Interactions of dihydroxybenzenes with the Ca^{2+}-ATPase: separate binding sites for dihydroxybenzenes and sesquiterpene lactones, Biochemistry 34 (1995) 14385–14393.
[28] F. Plenge-Tellechea, F. Soler, F. Fernandez-Belda, On the inhibition mechanism of sarcoplasmic or endoplasmic reticulum Ca^{2+}-ATPases by cyclopiazonic acid, J. Biol. Chem. 272 (1997) 2794–2800.
[29] S.R. Denmeade, J.T. Isaacs, The SERCA pump as a therapeutic target: making a "smart bomb" for prostate cancer, Cancer Biol. Ther. 4 (2005) 14–22.
[30] S.R. Denmeade, C.M. Jakobsen, S. Janssen, S.R. Khan, E.S. Garrett, H. Lilja, S. B. Christensen, J.T. Isaacs, Prostate-specific antigen-activated thapsigargin prodrug as targeted therapy for prostate cancer, J. Natl. Cancer Inst. 95 (2003) 990–1000.
[31] J. Isaacs, New strategies of the medical treatment of prostate cancer, BJU Int. 96 (2005) 35–40.
[32] A. Jaskulska, A.E. Janecka, K. Gach-Janczak, Thapsigargin - from traditional medicine to anticancer drug, Int. J. Mol. Sci. 22 (2020).
[33] C. Montigny, M. Picard, G. Lenoir, C. Gauron, C. Toyoshima, P. Champeil, Inhibitors bound to Ca^{2+}-free sarcoplasmic reticulum Ca^{2+}-ATPase lock its transmembrane region but not necessarily its cytosolic region, revealing the flexibility of the loops connecting transmembrane and cytosolic domains, Biochemistry 46 (2007) 15162–15174.
[34] R. Aguayo-Ortiz, L.M. Espinoza-Fonseca, Linking biochemical and structural states of SERCA: achievements, challenges, and new opportunities, Int. J. Mol. Sci. 21 (2020) 4146.

[35] C. Toyoshima, F. Cornelius, New crystal structures of PII-type ATPases: excitement continues, Curr. Opin. Struct. Biol. 23 (2013) 507–514.
[36] L. Yatime, M.J. Buch-Pedersen, M. Musgaard, J.P. Morth, A.M. Lund Winther, B. P. Pedersen, C. Olesen, J.P. Andersen, B. Vilsen, B. Schiott, M.G. Palmgren, J. V. Moller, P. Nissen, N. Fedosova, P-type ATPases as drug targets: tools for medicine and science, Biochim. Biophys. Acta 1787 (2009) 207–220.
[37] B. Yang, M. Zhang, J. Gao, J. Li, L. Fan, G. Xiang, X. Wang, X. Wang, X. Wu, Y. Sun, X. Wu, G. Liang, Y. Shen, Q. Xu, Small molecule RL71 targets SERCA2 at a novel site in the treatment of human colorectal cancer, Oncotarget 6 (2015) 37613–37625.
[38] T.T. Dao, P. Sehgal, T.T. Tung, J.V. Moller, J. Nielsen, M. Palmgren, S. B. Christensen, A.T. Fuglsang, Demethoxycurcumin is a potent inhibitor of P-type ATPases from diverse kingdoms of life, PLoS One 11 (2016) e0163260.
[39] F. Payton, P. Sandusky, W.L. Alworth, NMR study of the solution structure of curcumin, J. Nat. Prod. 70 (2007) 143–146.
[40] C. Toyoshima, M. Nakasako, H. Nomura, H. Ogawa, Crystal structure of the calcium pump of sarcoplasmic reticulum at 2.6 A resolution, Nature 405 (2000) 647–655.
[41] C. Toyoshima, T. Mizutani, Crystal structure of the calcium pump with a bound ATP analogue, Nature 430 (2004) 529–535.
[42] C. Olesen, M. Picard, A.M. Winther, C. Gyrup, J.P. Morth, C. Oxvig, J.V. Moller, P. Nissen, The structural basis of calcium transport by the calcium pump, Nature 450 (2007) 1036–1042.
[43] A. Volkamer, A. Griewel, T. Grombacher, M. Rarey, Analyzing the topology of active sites: on the prediction of pockets and subpockets, J. Chem. Inf. Model. 50 (2010) 2041–2052.
[44] G.M. Verkhivker, D. Bouzida, D.K. Gehlhaar, P.A. Rejto, S. Arthurs, A.B. Colson, S. T. Freer, V. Larson, B.A. Luty, T. Marrone, P.W. Rose, Deciphering common failures in molecular docking of ligand-protein complexes, J. Comput. Aided Mol. Des. 14 (2000) 731–751.
[45] C.R. Corbeil, C.I. Williams, P. Labute, Variability in docking success rates due to dataset preparation, J. Comput. Aided Mol. Des. 26 (2012) 775–786.
[46] M. Lape, C. Elam, M. Versluis, R. Kempton, S. Paula, Molecular determinants of sarco/endoplasmic reticulum calcium ATPase inhibition by hydroquinone-based compounds, Proteins 70 (2008) 639–649.
[47] C.M. Jakobsen, S.R. Denmeade, J.T. Isaacs, A. Gady, C.E. Olsen, S.B. Christensen, Design, synthesis, and pharmacological evaluation of thapsigargin analogues for targeting apoptosis to prostatic cancer cells, J. Med. Chem. 44 (2001) 4696–4703.
[48] Y. Cheng, W.H. Prusoff, Relationship between the inhibition constant (K1) and the concentration of inhibitor which causes 50 per cent inhibition (I50) of an enzymatic reaction, Biochem. Pharmacol. 22 (1973) 3099–3108.
[49] P. Sehgal, C. Olesen, J.V. Moller, Tryptophan fluorescence changes related to Ca^{2+}-ATPase function, Methods Mol. Biol. 1377 (2016) 227–230.
[50] K. Obara, N. Miyashita, C. Xu, I. Toyoshima, Y. Sugita, G. Inesi, C. Toyoshima, Structural role of countertransport revealed in Ca^{2+} pump crystal structure in the absence of Ca^{2+}, Proc. Natl. Acad. Sci. USA 102 (2005) 14489–14496.
[51] K. Moncoq, C.A. Trieber, H.S. Young, The molecular basis for cyclopiazonic acid inhibition of the sarcoplasmic reticulum calcium pump, J. Biol. Chem. 282 (2007) 9748–9757.
[52] G. Inesi, H. Ma, D. Lewis, C. Xu, Ca^{2+} occlusion and gating function of Glu309 in the ADP-fluoroaluminate analog of the Ca^{2+}-ATPase phosphoenzyme intermediate, J. Biol. Chem. 279 (2004) 31629–31637.
[53] L.L. Wootton, F. Michelangeli, The effects of the phenylalanine 256 to valine mutation on the sensitivity of sarcoplasmic/endoplasmic reticulum Ca^{2+} ATPase (SERCA) Ca^{2+} pump isoforms 1, 2, and 3 to thapsigargin and other inhibitors, J. Biol. Chem. 281 (2006) 6970–6976.
[54] R.L.M. van Montfort, P. Workman, Structure-based drug design: aiming for a perfect fit, Essays Biochem. 61 (2017) 431–437.